REPORT DOCUMENTATION PAGE

AFRL-SR-BL-TR-00-

0570

1. REPORT DATE (DD-MM-YYYY)	2. REPORT TYPE	3. DATES COVERED (From - To)
06/10/2000	FINAL	1996 - 2000

4. TITLE AND SUBTITLE
SYSTEMATIC OPTIMIZATION OF SECOND-ORDER NONLINEAR OPTICAL MATERIALS

5a. CONTRACT NUMBER
F49620-96-1-0295

5b. GRANT NUMBER
F49620-96-1-0295

5c. PROGRAM ELEMENT NUMBER

6. AUTHOR(S)
SETH R. MARDER

5d. PROJECT NUMBER

5e. TASK NUMBER

5f. WORK UNIT NUMBER

7. PERFORMING ORGANIZATION NAME(S) AND ADDRESS(ES)

UNIVERSITY OF ARIZONA
DEPARTMENT OF CHEMISTRY
TUCSON, AZ 85721

ALSO ORIGINALLY AT
CALIFORNIA INSTITUTE OF TECH-
NOLOGY
PASADENA, CA 91125

8. PERFORMING ORGANIZATION REPOR NUMBER

9. SPONSORING / MONITORING AGENCY NAME(S) AND ADDRESS(ES)

AFOSR/NL
801 North Randolph St, Rm 732
Arlington, VA 22203-1977

10. SPONSOR/MONITOR'S ACRONYM(S)
AFOSR

11. SPONSOR/MONITOR'S REPORT NUMBER(S)

12. DISTRIBUTION / AVAILABILITY STATEMENT

APPROVED FOR PUBLIC RELEASE: DISTRIBUTION UNLIMITED

13. SUPPLEMENTARY NOTES

Several key advances have been made. In the field of photorefractive polymers, a new molecule was developed which resulted in photorefractive composites with unprecedented performance both in the visible and the near infrared regions of the electromagnetic spectrum. In the field of organic light emitting diodes several new barrelene molecules have been made, including some which are water soluble and can be used in schemes for self-assembling light emitting diodes. In addition, molecules with tunable ionization potentials that can be incorporated into photocrosslinkable polymers have been synthesized. In the field of two-photon absorption, molecules that initiate polymerization have been characterized in terms of their efficiencies relative to commercial photoinitiators and have been shown to have much higher efficiencies and new electron deficient molecules based upon dioxoborine heterocycles have been synthesized and characterized. Finally, new dopants with large dielectric anisotropies have been synthesized in order to lower the switching voltage for liquid crystal mixtures. Several undergraduate and graduate students received an interdisciplinary training in materials synthesis and characterization.

15. SUBJECT TERMS

Nonlinear Optical, polymers

16. SECURITY CLASSIFICATION OF:			17. LIMITATION OF ABSTRACT	18. NUMBER OF PAGES	19a. NAME OF RESPONSIBLE PERS
a. REPORT	b. ABSTRACT	c. THIS PAGE			Seth R. Marder
Unclas	Unclas	Unclas		39	19b. TELEPHONE NUMBER (include a code) 520-574-0456 x 13

FINAL TECHNICAL REPORT FOR:

SYSTEMATIC OPTIMIZATION OF SECOND-ORDER NONLINEAR OPTICAL MATERIALS

Seth R. Marder

University of Arizona
Department of Chemistry and Optical Science Center
Science and Technology Park
Tucson, AZ 85747

AFOSR GRANT # F49620-96-1-0295

2. OBJECTIVES

The objectives of this program are to develop optical materials which may be used for applications including electro-optic modulators based upon poled polymers, device employing photorefractive polymers, improved chromophores for liquid crystal displays, polymerization utilizing two photon absorption and organic light emitting diodes (OLEDs) using conjugated organic polymers.

3. STATUS OF EFFORT

Several key advances have been made. In the field of photorefractive polymers, a new molecule was developed which resulted in photorefractive composites with unprecedented performance both in the visible and the near infrared regions of the electromagnetic spectrum. In the field of organic light emitting diodes several new barrelene molecules have been made, including some that are water soluble and can be used in schemes for self-assembling light emitting diodes. In addition, molecules with tunable ionization potentials that can be incorporated into photocrosslinkable polymers have been synthesized. In the field of two-photon absorption, molecules that initiate polymerization have been characterized in terms of their efficiencies relative to commercial photoinitatiors and have been shown to have much higher efficiencies. New electron deficient molecules based upon dioxoborine heterocycles have been synthesized and characterized. Finally, new dopants with large dielectric anisotropies have been synthesized in order to lower the switching voltage for liquid crystal mixtures. Several undergraduate and graduate students received interdisciplinary training in materials synthesis and characterization.

4. ACCOMPLISHMENTS AND NEW FINDINGS

4.1 Synthesis of Precursors and Polymers for OLEDs

Michael Wagaman, graduate student working under the direction of Professor Robert H. Grubbs.

4.1.1 Results

The ring opening metathesis polymerization (ROMP) synthetic route to poly-paraphenylene-vinlyenes requires the synthesis of substituted barrelenes. Several diester substituted barrelenes have been synthesized and characterized as shown below (Scheme 4.1.1.1).

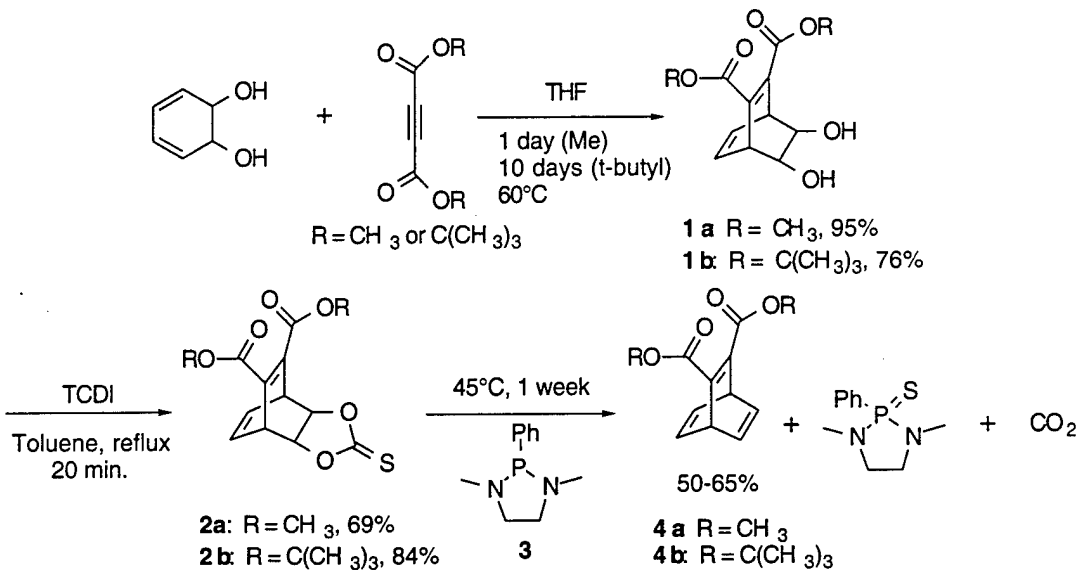

Scheme 4.1.1.1

Also the synthesis, characterization and photoluminescence (PL) studies of conjugated polymers and conjugated water soluble polymers made from these materials has been completed (Scheme 4.1.1.2).

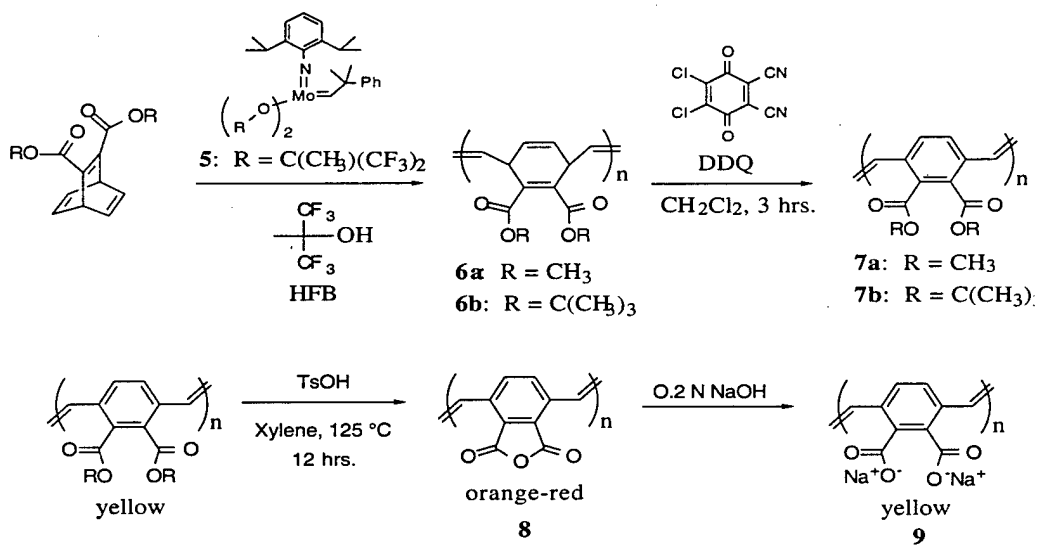

Scheme 4.1.1.2

Some of this work has been reported [Wagaman, M. W. and Grubbs, R. H. *Macromolecules*, **30**, 3978 (1997)]. Samples of the above materials are currently under study for the fabrication of electroluminescent devices by Nassar Peyghambarian's group at the University

of Arizona and by Mark Thompson's group (study of monolayer deposition of polyanion samples) at USC.

In addition, other substituted barrelene monomers have been synthesized that incorporate electron withdrawing substituents, as shown below (Scheme 4.1.1.3). Details of this synthesis are included in a paper in the *Journal of Organic Chemistry.*

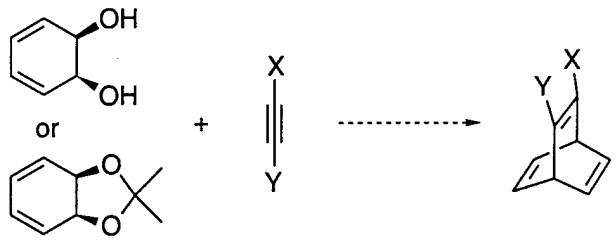

X = Y = CO_2R; X = Y = CF_3; X = CF_3, Y = $(CF_2)_7CF_3$;
X = Y = H; X = H, Y = $(CH_2)_7CH_3$

Scheme 4.1.1.3

Several copolymers of diester-polyphenylenevinylene/polynaphthalenevinylenes have been synthesized for further study of electroluminescence properties by Nassar Peyhgambarian's group (Scheme 4.1.1.4). Photoluminescence of these materials shows electron/hole transport in films, so the same transport should be observed in the electroluminescence as well. Photoluminescence of the random copolymer shows the average emission wavelength maximum of the two homopolymers.

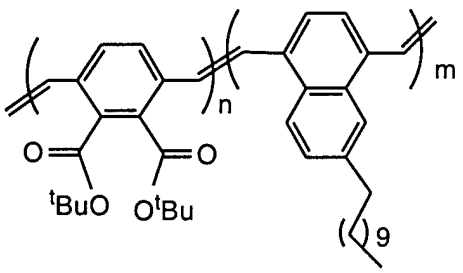

Scheme 4.1.1.4

The synthesis of conjugated/unconjugated block copolymers and water soluble/water insoluble (organic soluble) block copolymers has been undertaken. The first block copolymer was made with norbornene and the diester barrelene (Scheme 4.1.1.5). This required doing the first block in neat tetrahydrofuran (THF) (with hexafluoro *t*-butanol (HFB), added to activate the

catalyst) to allow complete initiation of the first block of the polymerization). The second block, the barrelene block, was then polymerized by first removing the THF and then doing the polymerization in a mixture of benzene and a little HFB (Scheme 4.1.1.5). These conditions allowed complete initiation of both blocks and reasonable polymerization times. However, the norbornene block decomposed on attempts at aromatizing the barrelene block (Scheme 4.1.1.5).

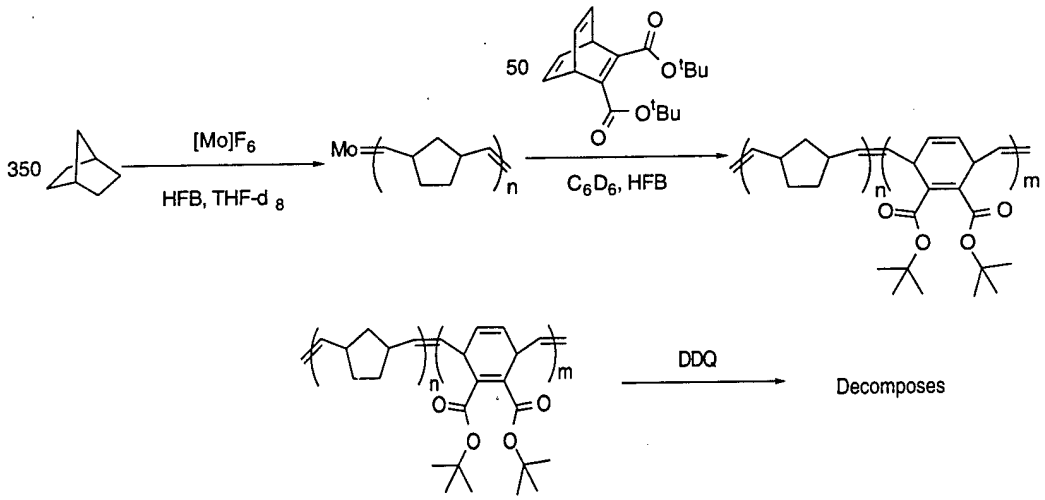

Scheme 4.1.1.5

To avoid decomposition, block copolymers of the diester barrelene and benzobarrelene were made with trichlorobenzobarrelene, which requires higher temperatures to become aromatized (typically heating overnight in toluene at 110°C is required) (Scheme 4.1.1.6).

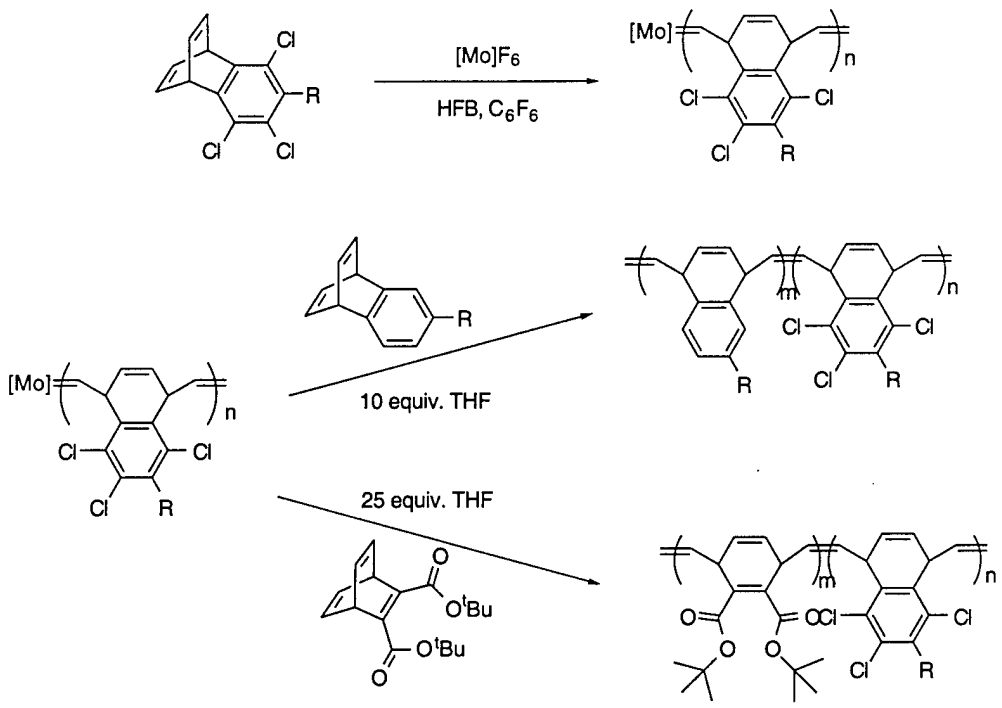

Scheme 4.1.1.6

Exposure of these materials to dicyanodichloroquinone (DDQ) in methylene chloride at room temperature selectively aromatizes the diester barrelene or undecyl-barrelene block (Scheme 4.1.1.7). To identify other materials for the synthesis of these types of block copolymers, polyimide ROMP homopolymers were exposed to DDQ under the conditions typically used for aromatization of the diester-PPV and undecyl-PNV. After 1 day in the presence of 1 equivalent of DDQ, the polymers showed minimal decomposition as shown by ^1H NMR and by comparison of the polymers' GPC traces before and after this exposure. Although slight decomposition was observed, as shown by a low molecular weight tail in the GPC, less decomposition would be expected for the copolymers since the DDQ would be consumed by aromatization of the other block. In the case of the undecyl-PNV prepolymer, aromatization and therefore consumption of DDQ occurs almost instantly. In the case of the BC-PPV prepolymer, the reaction is nearly complete after 3 hours.

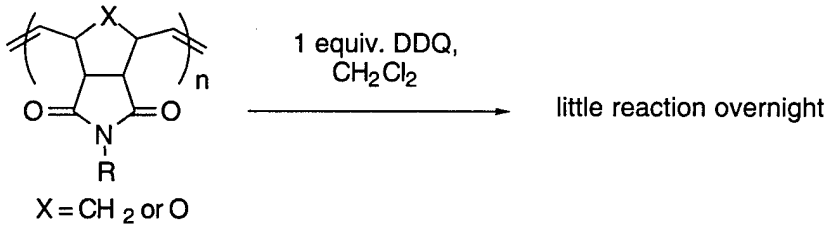

Scheme 4.1.1.7

4.2 Fabrication of Three-Dimensional Structures Using Two-Photon Initiated Polymerization and Studies of the Polymerization Kinetics

4.2.1. Introduction

Ms. Lael Erskine, Undergraduate student at Caltech, working under the direction of Dr. Joseph W. Perry.

Molecules exhibiting strong two-photon absorption hold great potential for a wide range of applications including: two-photon fluorescence imaging, three-dimensional (3D) optical data storage, 3D microfabrication, photorefraction and optical limiting. We have observed large two-photon absorptivities in bis-donor diphenylpolyene derivatives, that are correlated to simultaneous charge transfers from the end groups to the polyene bridge in the molecule. These molecules are also excellent photoexcitable electron donors that can initiate charge-transfer reactions. In initial applications of these materials we have demonstrated their use in two-photon initiation of polymerization and optical limiting.

Two-photon initiated polymerization holds tremendous promise for ultrahigh density optical memory and 3D microfabrication. One can selectively polymerize very small volumes of polymer near the focus of a laser beam, thus creating a change in refractive index and permitting data storage densities of 10^{12} bits/cm.[1] The bis-donor diphenylpolyenes are excellent electron donors and we have shown that upon excitation they are able to initiate polymerization of acrylate monomers and multifunctional acrylates. These materials have allowed us to develop a new class of two-photon writable photopolymers that have high writing speed as a result of their large two-photon absorptivity. The two-photon photopolymer blends are comprised of 1) a two-photon absorbing initiator, 2) a crosslinkable monomer, and 3) a polymer binder. With these new two-photon photopolymers, we have written micrometer dimension crosslinked polymer spots in two- and three-dimensional patterns. We are currently exploring the use of these new photopolymers for 3D microfabrication. As part of a Summer Undergraduate Research Fellowship, supported by the BMDO AASERT program, Ms. Erskine performed studies of the rates of two-photon initiated polymerization of triacrylate monomers by bis-donor substituted diphenylpolyenes and utilized photopolymer systems based on combinations of such materials to fabricate features of crosslinked polymers by two-photon writing, as discussed below.

4.2.2 Results

Pulsed laser studies of rates of two-photon initiated polymerization.

Systematic studies of the growth rates of polymer features formed by two-photon excitation were performed as a function of laser intensity and exposure time for various initiators. The initiators were dissolved in a commercial triacrylate monomer (Sartomer, SR9008). For these studies the concentration of initiator was held constant at 0.025 M and 5-ns, 596 nm laser pulses were used for excitation. Studies were performed in the presence and absence of inhibitor, which provided cases of high and low termination rates, respectively. The optical cells used for the initiation studies were comprised of two glass windows that were clamped together and separated by an o-ring seal. The interior surface of one of the windows, the one on which the laser beam was incident, was treated with an aminosilane coupling agent to promote adhesion of the crosslinked polymer to the window. Two dimensional arrays of cylindrical crosslinked polymer features, for which the intensity of exposure was varied along one direction and the time of exposure was varied along the other direction, were produced. After exposures were completed, the cells were opened and the written features, which were attached to the treated window, were washed with tetrahydorfuran and dried. The crosslinked polymer features were then imaged using scanning electron microscopy (SEM). The volumes of the written features were calculated from dimensions obtained from the SEM images. The initial slopes of plots of the polymerized volumes as a function of exposure time were calculated and taken as proportional to the rate of polymerization. For samples either with or without the inhibitor the termination rates were constant, thus the variation in the rates of polymerization reflect changes in the rate of initiation. For a two-photon initiation, the rate of polymerization should be proportional to the intensity, whereas for a one-photon process it is proportional to the square root of the intensity.

We investigated the relative rate of initiation for our bis-donor molecules as compared to the conventional initiators. The commercial photoinitiators examined for two-photon initiation were: 2,2-diethoxy-2-phenyl acetophenone (UV1), benzil (UV2), benzoin ethyl ether (UV3), benzophenone (UV4), 4,4' bis(dimethylamino)benzophenone (UV5), dl-camphorquinone (UV6), 2-methyl-4'(methylthio)-2-morpholino propiophenone (UV7), 2-isopropyl-9H-thioxanthen-9-one (UV8), 4,4'-bis(dimethylamino)benzil (UV9). Tables 4.2.2.1 and 4.2.2.2 summarize our observations for samples without and with inhibitor, respectively.

Table 4.2.2.1. Two-photon polymerization thresholds and rates for triacrylate monomer without inhibitor and various initiators (commercial photoinitiators or p,p'-bis-di-n-butylaminostilbene (BDAS)). Laser excitation at 596 nm, spot size ~150 μm. Rates are given for exposures of ~1.25 mJ/pulse and 20 pulses/sec. Under the comments column, gelled indicates that the whole monomer volume solidified prior to disassembly and washing, obviating SEM analysis.

Initiator	Comments	Threshold
UV1	did not write, gelled	> 4 mJ
UV2	wrote, gelled	~0.4 mJ
UV3	did not write	> 4.75 mJ
UV4	did not write	> 4.75 mJ
UV5	wrote a little, gelled	~1mJ
UV6	wrote a little, gelled	~3.2 mJ
UV7	wrote, gelled	~0.5mJ
UV8	wrote a little	1 mJ (rate = 3 x 10^5 μm^3/sec)
UV9	did not write	> 3 mJ
BDAS	wrote	0.3 mJ (rate = 31 x 10^5 μm^3/sec)

Table 4.2.2.2. Two-photon polymerization thresholds and rates for triacrylate monomer with inhibitor and various initiators (commercial photoinitiators or p,p'-bis-di-n-butylaminostilbene (BDAS)). Laser excitation at 596 nm, spot size ~150 μm, data for samples without inhibitor. Rates are given for exposures of ~1.25 mJ/pulse and 20 pulses/sec. Under the comments column, gelled indicates that the whole monomer volume solidified prior to disassembly and washing, obviating SEM analysis.

Initiator	Comments	Threshold
UV2	wrote very little	~0.6 mJ
UV5	wrote a little	~1.0 mJ (rate = 2.5 x 10^5 μm^3/sec)
UV6	wrote a little, gelled	~0.6 mJ
UV7	wrote	~1.1mJ (rate = 6.1 x 10^5 μm^3/sec)
BDAS	wrote	0.38 mJ (rate = 8.4 x 10^5 μm^3/sec)

Without inhibitor, UV1, UV3, UV4, and UV 9 did not initiate polymerization even at laser pulse energies of 3 to 4.75 mJ. UV2, UV5, UV7, and UV8 initiated polymerization and exhibited thresholds of 0.4 to 1 mJ. Several of the commercial photoinitiators led to samples that gelled, likely due to ambient light initiation, making these samples difficult to process for microfabrication. BDAS initiated effectively with a threshold of 0.3 mJ and did not lead to gelling of the sample. More importantly the rate of initiation for BDAS was ten times higher than for UV8. In the presence of inhibitor, BDAS was again the most effective and useful initiator, having the lowest threshold and highest polymerization rate. UV7 was also reasonably effective and useful, as a two-photon initiator, in that the samples did not gel.

Table 4.2.2.3 summarizes a comparison of the rates of polymerization for a series of bis-donor diphenylpolyenes. For the series of compounds, that include diamino and amino-alkoxy compounds with one and two linking double bonds, BDAS exhibited the highest rate of polymerization. We know from nonlinear transmission measurements that BDAS has a two-photon absorption peak at about 600 nm, consistent with the high initiation efficiency. The p-diethylamino, p'-butoxystilbene molecule shows a much lower initiation rate, consistent with the much weaker two-photon absorption at the excitation wavelength observed in nonlinear transmission measurements. Also p-dimethylamino, p'-di-n-butylaminodiphenylbutadiene shows a significantly lower rate of polymerization and we know that the two-photon absorption is red shifted relative to BDAS and the two-photon absorption at 596 is weaker than for BDAS. Interestingly, for p-dibutylamino, p'-methoxydiphenylbutadiene the polymerization rate has increased relative to p-diethylamino, p'-di-n-butylaminostilbene, consistent with a red shift that brings the two-photon absorption into resonance with the 596 nm excitation wavelength.

Table 4.2.2.3. Rates of two-photon polymerization for triacrylate monomer, with inhibitor, initiated by bis-donor diphenylpolyenes with 596 nm, 1.25 mJ/pulses and 20 pulses/sec.

Molecule	Rate of Polymerization (10^5 μm^3/sec)
p,p'-bis-di-n-butylaminostilbene (BDAS)	8.4
p-diethylamino, p'-di-n-butylaminostilbene	5.7
p-diethylamino, p'-butoxystilbene	2.0
p-dibutylamino, p'-methoxydiphenylbutadiene	4.5
p-dimethylamino, p'-di-n-butylaminodiphenylbutadiene	2.8

For the bis-donor substituted diphenylpolyenes examined, the intensity dependence of the rate of polymerization in most cases followed a linear dependence, as expected for a two-photon initiation. For molecules with very high initiation rates, such as bis-di-n-butylaminostilbene, the intensity

dependence in the absence of initiator showed a saturation effect. For molecules that showed very little initiation, such as many of the commercial initiators, the intensity dependence was highly scattered. More complete studies of the polymerization kinetics would include investigation of the excitation wavelength dependence and initiator concentration dependence.

We have hypothesized that the initiation of polymerization involves a two-photon excited charge transfer reaction between the bis-donor molecule and the monomer. Such a reaction would lead to the appearance of the radical cation of the bis-donor molecule, whose electronic absorption has been determined by using spectroelectrochemical methods. In order to build up a sufficiently large concentration of radical cations, we performed an experiment using UV single-photon excitation of the bis-donor molecule; UV light is absorbed very efficiently by the molecules. Indeed, on prolonged UV exposure of triacrylate monomers containing bis-di-n-butylaminostilbene, we observed a build up of a green coloration of the sample. Spectral measurements reveal an absorption band, a sharp band near 600 nm, very similar to that observed for the radical cation by spectroelectrochemistry. This indicates the formation of the initiator radical cation during photopolymerization and is consistent with the hypothesis.

4.3 Synthesis of NLO chromophores for electro-optic applications.

Jeffrey Mendez, undergraduate student at Caltech, working under the direction of Dr. Seth R. Marders

4.3.1 Introduction

To make electro-optic materials, the NLO chromophores are incorporated into polymers as a host-guest system or they are covalently attached to the polymer backbone. Covalent incorporation of the NLO chromophores is preferred over the host-guest system, since: (1) sublimation of the NLO chromophores is obviated when they are covalently incorporated into the polymeric system. (2) processibility problems due to phase separation at high loading is less likely with covalently incorporated systems.

Covalent incorporation of NLO chromophores into polymers can be achieved by using functionalized NLO chromophores as co-monomers in the polymerization reaction or by attaching the chromophores to a prefunctionalized polymer under mild reaction conditions.[1] Since the former procedure involves survival of the NLO chromophores in the harsh polymerization reaction conditions, the later procedure is preferred. The later procedure involves incorporation of hydroxy functionalized chromophores into polymers with phenolic functionalities under Mitsunobu reaction conditions.[2]

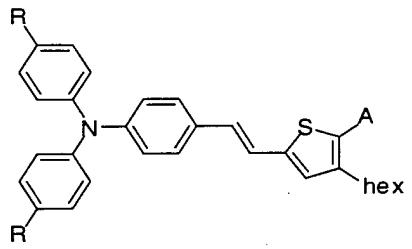

1

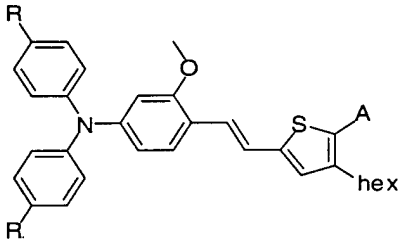

2

A = acceptor moiety

The dipole alignment in organic electro-optic materials is achieved by poling at temperatures above the glass transition temperature of the host polymer. Therefore, it is imperative that the NLO chromophores possess high thermal stabilities. It has been recently shown that substitution of diarylamino group as the donor in the place of dialkylamino group improves the thermal stabilities of the chromophores without a major compromise in optical nonlinearities. We have recently demonstrated that chromophores represented by structure **1** exhibit high optical nonlinearities with enhanced thermal and photochemical stabilities when compared to the corresponding dialkylamino donor based chromophores. In that paper, we also show that the incorporation of an additional methoxy group on the bridging phenyl ring (represented by **2**) enhances the optical nonlinearities without any major effect on their thermal and photochemical stabilities. Therefore, we chose to synthesize hydroxy alkyl functionalized chromophores represented by **2**.

4.3.2. Results and Discussion

We approached the syntheses of these chromophores in a convergent fashion. The functionalized triarylamine part of the chromophores were synthesized as TBS-protected hydroxyalkyl terminated (diarylamino)arylcarboxaldehyde **3**. The main skeleton of the chromophores was then assembled by a Wittig reaction with a thiophene phosphonium salt **6**. The acceptor was then installed in the last or the penultimate step of the synthesis.

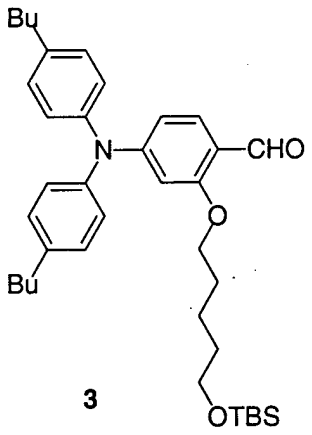

3

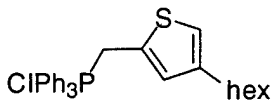

4

The triarylamines were assembled using the palladium catalyzed aryl carbon-nitrogen bond forming reaction reported in the literature recently.[3] The alkoxy functionalized triarylamine **3** was synthesized from the triarylamine **6**, which was assembled in 84% yield from *m*-anisidine and **5** under palladium catalysis conditions. The methoxy triarylamine **6** was converted to the phenol **7** by reaction with BBr_3 in 66% yield. Treatment of **7** with monoprotected pentane-1,5-diol **8** under Mitsonobu reaction conditions affords the product **9**. The synthetic sequence in shown in Scheme 4.3.2.1.

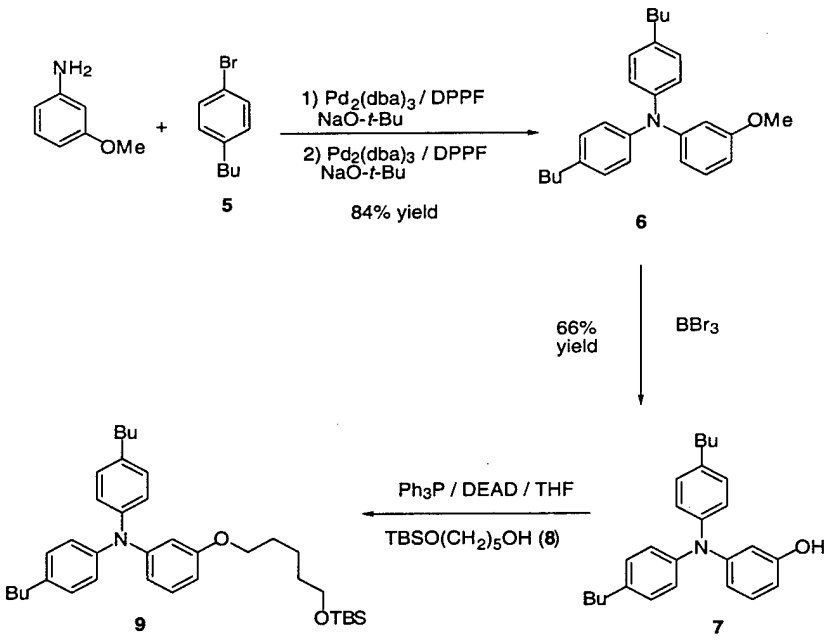

Scheme 4.3.2.1

Bromination of the open para- position in the triarylamine ring in **9** using *N*-bromosuccinimide in DMF provides the brominated triarylamine **10** in low yield. Bromine-lithium exchange and the subsequent treatment of the organolithium intermediate with DMF affords the triarylamine carboxaldehyde **3** in 14% overall yield from **7**.

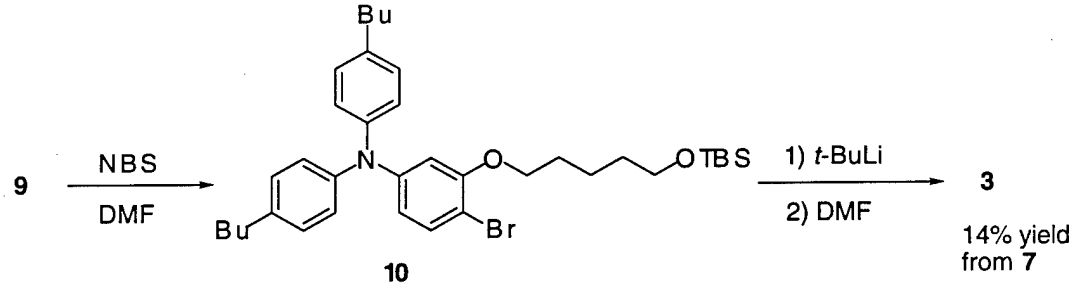

For the synthesis of 4-hexylthiophene-2-methylenetriphenylphosphonium chloride (**4**), we utilized the commercially available 4-bromothiophene-2-carboxaldehyde (**11**) as the starting material. Reduction of the aldehyde to the corresponding alcohol folowed by protection of the hydroxy group provided the 4-bromothiophenemethylene ether (**12**). At this juncture, the hexyl group was installed by nickel catalyzed coupling reactions to afford **13**. The methylene ether was then converted to the phosphonium salt **4**. The synthetic sequence is outlined in Scheme 4.3.2.2.

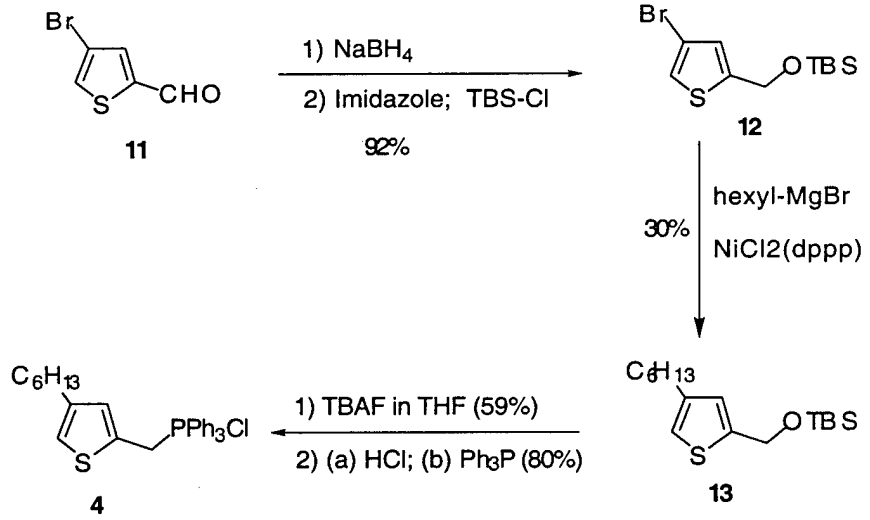

Scheme 4.3.2.2

Treatment of the aldehyde **3** with the phosphonium salt **4** under Wittig reaction conditions using sodium ethoxide as the base in ethanol affords the thiophenyl stilbene compound **14** as outlined below. The compounds were obtained as a mixture of cis- and trans isomers and these compounds were carried over to the next step without further manipulation.

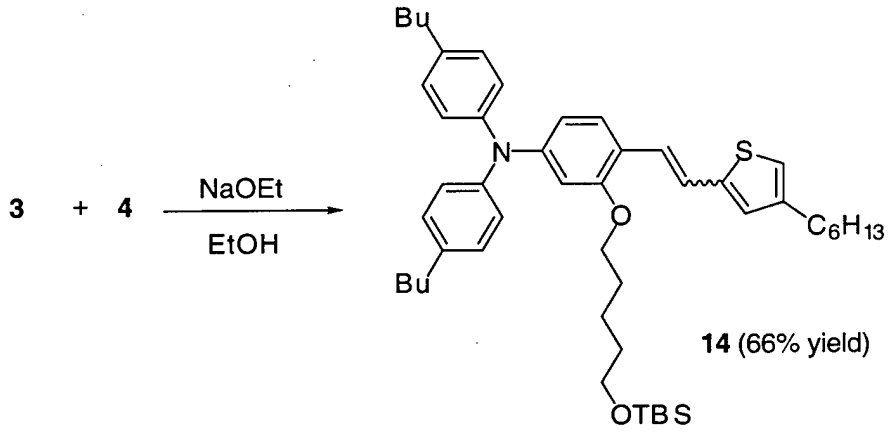

Treatment of the compound **14** with *n*-butyllithium followed by reaction with tetracyanoethylene affords the corresponding tricyanovinylated chromophore. Deprotection of the TBS-ether at this juncture using acetic acid affords the hydroxy functionalized tricyanovinylated chromophore **15**. The chromophore was obtained exclusively as a trans- isomer after the installation of the tricyanovinyl moiety in the structure. This result is attributed to the strength of the tricyanovinyl group as an acceptor that favors significant contribution from the charge-transfer structure. This offers the chromophore an opportunity to isomerize to the thermodynamically more stable trans isomer.

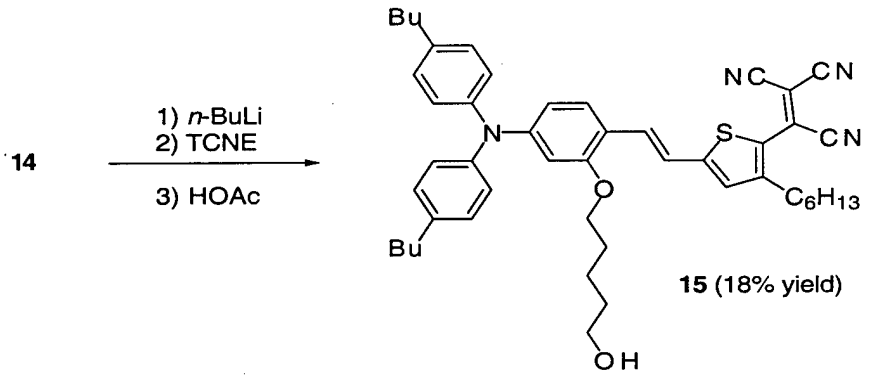

We also targeted functionalized chromophores with dicyanovinyl group as acceptor moiety. For this purpose, we treated the compound **14** with *n*-butyllithium followed by DMF to afford the aldehyde product **16** in 80% yield as a 6:4 mixture of trans and cis isomers. This mixture was then treated with aqeuous acetic acid in THF for 12 hours at room temperature and for another 12 hours at 45°C. At this time, in addition to the deprotection of the hydroxy group there was a partial isomerization to afford the hydroxy functionalized aldehyde product **17** in 88% yield as a 9:1 mixture of trans and cis isomers as shown below.

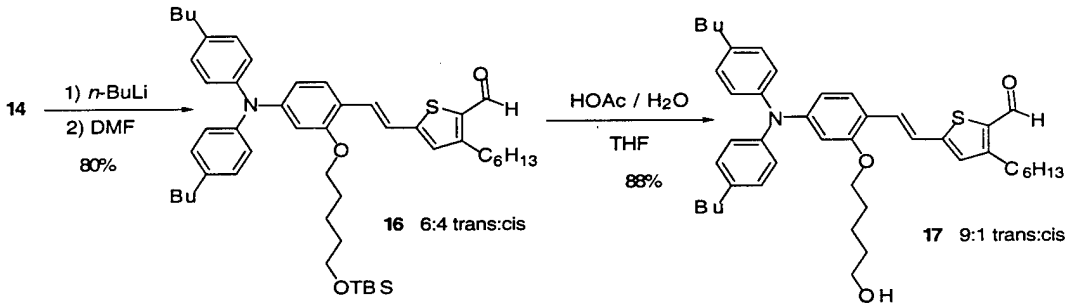

The aldehyde **17** was subjected to Knoevanagel reaction conditions with malononitrile to afford the chromophore **18**. The aldehyde was treated with malononitrile in methyelene chloride at room temperature in the presence of catalytic amount of triethylamine for 5 hours to obtain the chromophore **18** in 93% yield.

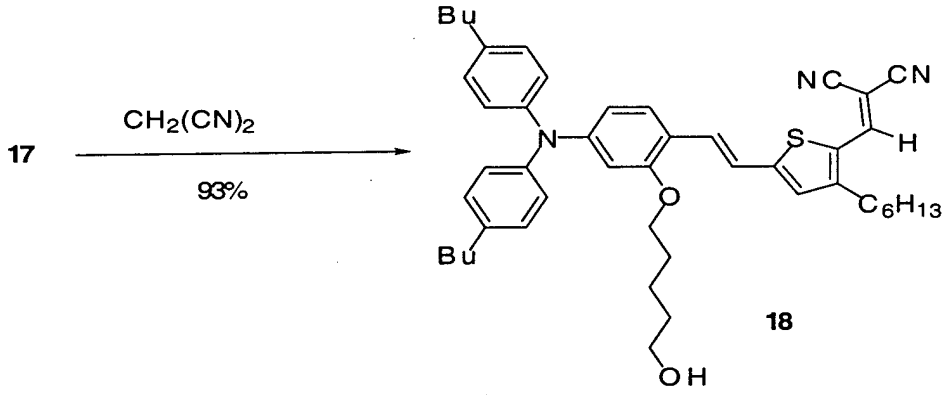

In summary, we designed and synthesized hydroxy alkyl functionalized chromophores with second order nonlinear optical properties. Since the corresponding unfunctionalized chromophores have been demonstrated to show high optical nonlinearities along with enhanced thermal and photochemical stabilities, we expect these chromophores to have similar properties associated with them. Work is in progress to study the properties of bulk electro-optic materials following incorporation of these chromophores into high performance polymers.

4.4 Synthesis and Properties of a Diarylaminoferrocene and its Radical Cation

Arjun Mendiratta, undergraduate student at Caltech, working under the direction of Dr. Seth R. Marder

4.4.1 Introduction

Amines, such as triarylmines, 4,4'-bis(diarylamino)biphenyls and carbazole derivatives, are of interest as hole-transport agents in xerography, light-emitting diodes and in photorefractive devices. We were interested in investigating the use of diarylaminoferrocenes for these applications. Previous routes to these compounds have been based upon Ullmann-type couplings of bromoferrocene and diarylamide anions. Ullmann couplings are notoriously variable in yield and the efficient synthesis of bromoferrocene requires the handling of environmentally hazardous chloromercuriferrocene. Therefore, we were interested in developing an alternative route to diarylaminoferrocenes. Recently, Pd-catalyzed routes to both diaryl- and triarylamines have been described; here we describe the application of this methodology to the synthesis of *N,N*-di-(*p*-tolyl)aminoferrocene (**1**). The properties of **1** and its one-electron oxidation product (**2**) are also described.

4.4.2 Results and Discussion

The Pd-catalyzed coupling of aminoferrocene and excess *p*-bromotoluene (Figure 4.4.2.1) under rigorously deoxygenated conditions gave **1** in yields similar to that reported for the Ullmann-type procedure for *N,N*-diphenylaminoferrocene. In the presence of oxygen, azoferrocene was found to be the major isolable product; the oxidation of aminoferrocene to azoferrocene under different conditions has previously been reported. Attempts to couple bromoferrocene and *p*-tolylamine were unsuccessful; these results are consistent with our previous studies of electron-rich aryl bromides. Thus, the Pd-catalysis route to *N,N*-diarylaminoferrocenes is complementary to the traditional Ullmann route in that aminoferrocene, rather than bromoferrocene, is the ferrocene source. The avoidance of bromoferrocene also has the advantage of circumventing the mercury chemistry used to synthesize bromoferrocene.

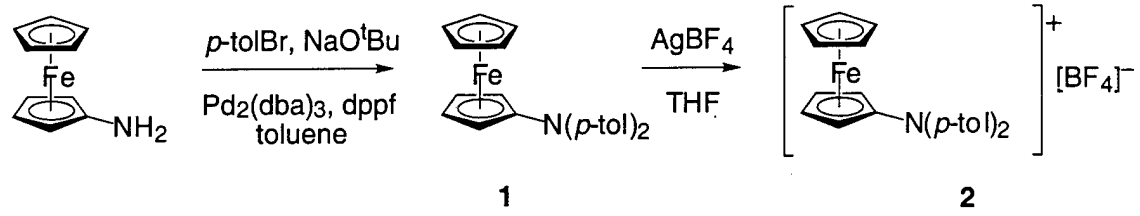

1 2

Figure 4.4.2.1. Synthesis of *N,N*-di-(*p*-tolyl)aminoferrocene (**1**); dba = dibenzylideneacetone, dppf = 1,1'-bis(diphenylphosphino)ferrocene.

1 has been characterized by elemental analysis, single crystal X-ray crystallography, ^{1}H and ^{13}C NMR spectrocsopy, and UV-vis. spectroscopy; the UV-vis. spectrum is essentially identical to the published spectrum of *N,N*-diphenylaminoferrocene. The electrochemistry of **1**, together with that of two other ferrocenyl nitrogen compounds, is summarized in Table 4.4.2.1. Figure 4.4.2.2 shows the cyclic voltammogram of **1**. Clearly **1** is considerably more susceptible to oxidation than ferrocene; for comparison, $Fe(C_5Me_4H)_2$ is oxidized at –360 mV vs. ferrocenium / ferrocene under the same conditions. Aminoferrocene is even more readily oxidized than **1**; presumably the nitrogen lone pair of $FcNH_2$ occupies a p-like orbital and can thus act as an effective donor to the ferrocene moiety, whilst that of **1** is more sp^3-like due to the steric demands of the aryl groups. Both $[\mathbf{1}]^+$ and the aminoferrocene cation undergo irreversible second oxidations at higher potential.

Table 4.4.2.1. Half-wave potentials vs. ferrocenium/ferrocene for three ferrocenes with nitrogen substituents, measured using cyclic voltammetry in THF (0.1 M $[^{n}Bu_4N]^+[PF_6]^-$) at a scan rate of 50 mVs^{-1}; Fc = ferrocenyl.

Compound	$E_{1/2}([m]^+ / [m])$ / mV	$E_{1/2}([m]^{2+} / [m]^+)$ / mV
1	–255	[a]E_{ox} = +715
$FcNH_2$	–405	[a]E_{ox} = +660
FcN=NFc	+110	+280

[a]Irreversible; peak potentials given.

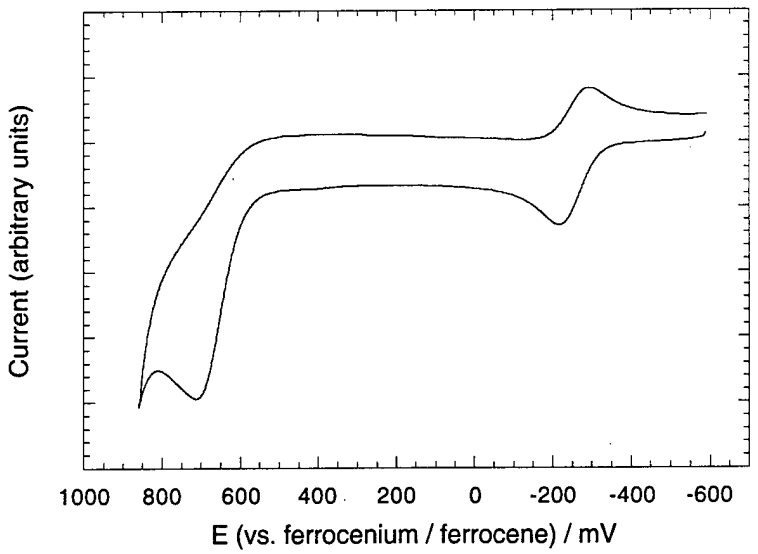

Figure 4.4.2.2. Cyclic voltammogram of **1** recorded in THF (0.1 M $[^nBu_4N]^+[PF_6]^-$) at a scan rate of 50 mVs^{-1}.

We chemically oxidized **1** to its tetrafluoroborate salt, **2**, using $AgBF_4$. The temperature dependence of the magnetic susceptibility of **2** obeys the Curie-Weiss law with a Curie constant of 0.546 emu K mol^{-1} and a Weiss constant of –0.32 K. The effective room temperature magnetic moment of 2.1 μB is consistent with an $S = {}^1/_2$ cation with an average g value ($\langle g \rangle$) of 2.4. This indicates that the positive charge is principally ferrocene-based; values of $\langle g \rangle$ for ferrocenium ions range between *ca.* 2.3 and *ca.* 2.8, whilst for amine-centered radical cations, one would anticipate an isotropic **g** tensor of *ca.* 2.00. The UV-vis.-NIR spectrum of **2** is shown in Figure 4.4.2.3. The lowest energy absorption maximum occurs at 1026 nm in dichloromethane (983 nm in acetonitrile). This maximum is considerably red-shifted from that of the unsubstituted ferrocenium ion (745 nm in acetonitrile); similar red-shifts have been noted for arylferrocenium ions with electron-donating groups in the *para* position. This is consistent with the assignment of the low energy band of the ferrocenium ion as a ligand-metal charge-transfer.

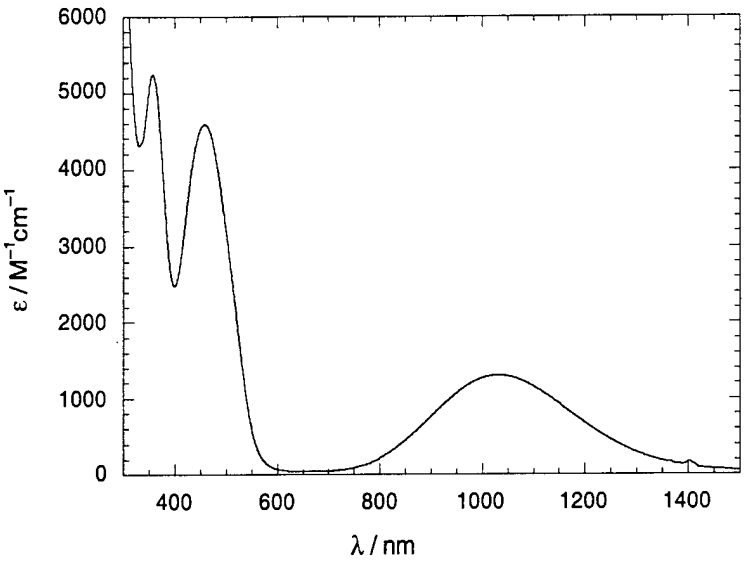

Figure 4.4.2.3. UV-vis.-NIR spectrum of **2** in dichloromethane.

4.4.3. Summary

The recently discovered palladium-catalyzed C—N bond-formation reaction can readily be applied to aminoferrocene substrate. By comparison with previous studies on triarylamine synthesis, it should be possible to synthesize *N,N*-diarylaminoferrocene derivatives bearing a wide variety of substituents. *N,N*-Di-(*p*-tolyl)aminoferrocene is a rather easily oxidized ferrocene derivative; *N,N*-diarylaminoferrocenes may therefore be of interest as components of magnetic materials and as non-linear optical chromophores. The hole transport properties of thin films of *N,N*-diarylaminoferrocenes may also be of interest.

4.5 Development of Structure-Property Relationships for Two-Photon Absorbing Molecules Based upon a Dioxaborine Heterocycle Motif and the Examination of Dioxaborine Heterocycles for Electron Transport Materials

Cara Grasso, graduate student working under the direction of Dr. Seth R. Marder.

4.5.1 Synthesis

Dioxaborine heterocycles (DOB's) of the general structure **1** shown below in Figure 4.5.1 are 1:1 chelate complexes formed from enolizable 1,3-diketones and boronic acid derivatives or

halogens. The boron atom fixes a negative charge so the π-system of the dicarbonyl ligands is positively charged. These types of complexes have some remarkable properties, e.g., they are strong π-electron acceptors, exhibit strong absorptivity, high thermal stability and in contrast to complexes with heavy metal ions, they have a strong fluorescence both in solution and solid state. Due to these combination of properties, dioxaborine heterocycles could be interesting, in combination with donor substituted systems as charge transfer systems for optical limiting and as A-π-A or D-A-D systems in two-photon absorbing sensitizers photorefractive polymers.

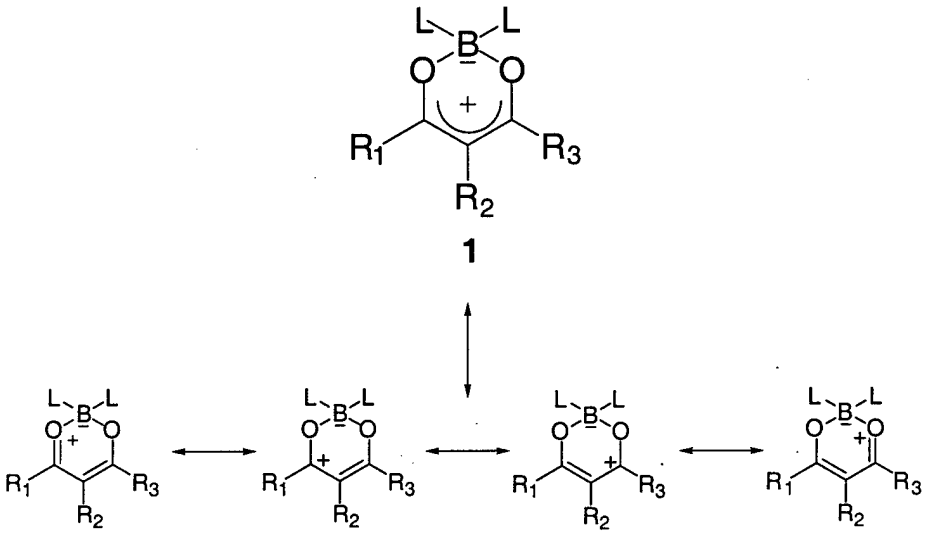

1

Figure 4.5. 1.1.

A meta, para dimethoxypenyl diketone **CG23** was synthesized to study the effect that the meta methoxy would have on the solubility and fluorescence of the dioxaborine. A condensation reaction was performed as shown in Scheme 4.5.2 to yield 11.363 g (40%) of the diketone. A small sample of the diketone was reacted with boron trifluoride to give the dioxaborine **CG24**. The product was a bright orange solid which was recrystallized from acetic anhydride. The product was fluorescent in dichloromethane and in the solid state.

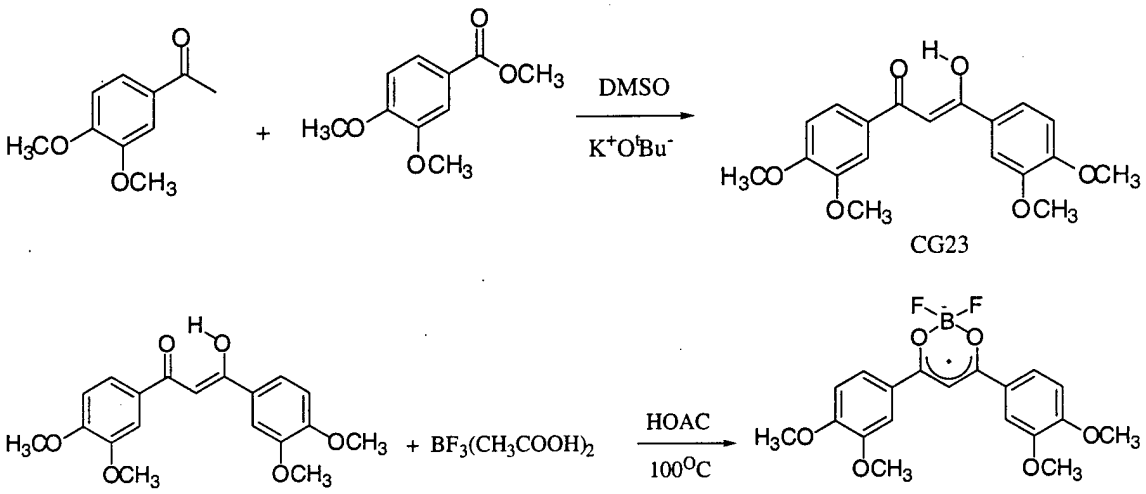

Scheme 4.5.1.2

The diketone **CG23** was also reacted with boric acid and oxalic acid to give the oxalyl dioxaborine **CG26** as shown in scheme 4.5.1.2. This was also a bright orange solid.

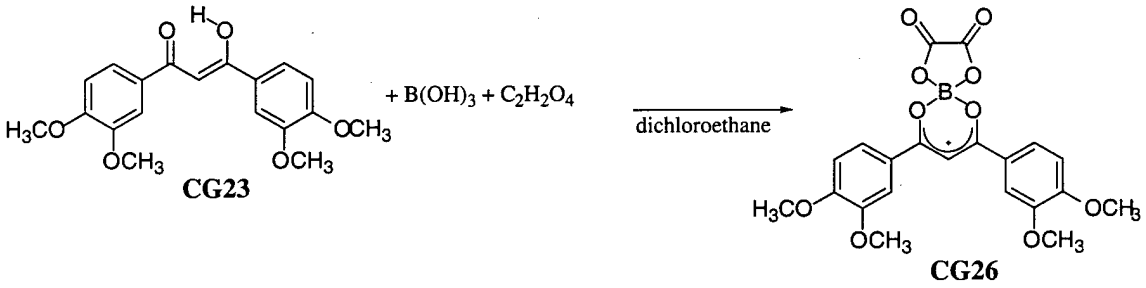

Scheme 4.5.1.3

The trimethoxydiketone **CG32** was synthesized in the same manner as the dimethoxydiketone. The diketone was reacted with boron trifluoride in acetic acid for 20 minutes at 100°C to make **CG34** that was a yellow solid (scheme 4.5.1.3). The product was recrystallized from acetic acid.

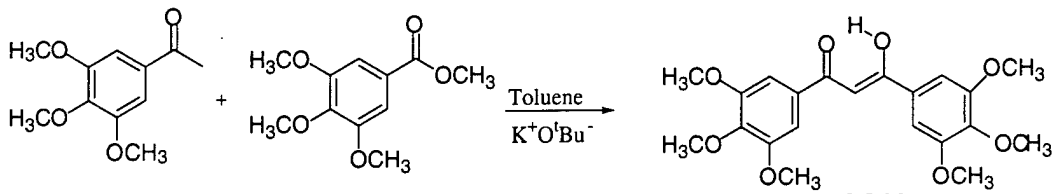

CG32

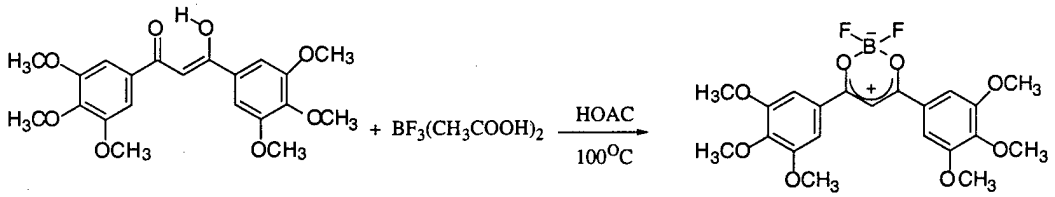

CG32 CG34

Scheme 4.5.1.3

The oxalic substituted oxaborine **CG35** was also synthesized from the trimethoxy diketone.

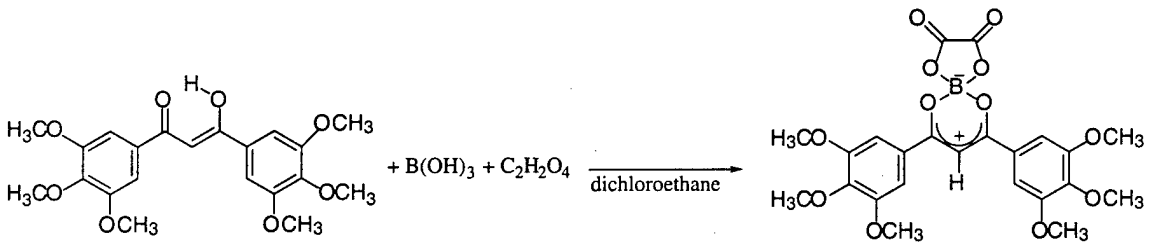

CG32 CG35

Scheme 4.5.1.4

This group of compounds was quite fluorescent in solution and in the solid state. The extinction coefficients range from 48000 to 54000 L/mol*cm as summarized in Table 4.5.1.1. Changing the ligands on the boron from fluoride to oxalyl shifts the wavelength of maximum absorption approximately 25 nm toward the red. The addition of the third methoxy group shifts the absorption maximum to lower wavelength by about 9 nm. The emission maxima of the trimethoxy compounds is at lower energy than the dimethoxy compound and the Stokes shift of the trimethoxy compound is much larger than the dimethoxy compounds

Table 4.5.1.1 Absorption and Emission Data

Compound	Extinction Coefficient (log ε)	Absorption Max (nm)	Emission Max. (nm)
CG24	4.74	432	475
CG26	N/A	458	498
CG34	4.71	423	510
CG35	4.68	449	533

4.5.2 Synthesis of Two-photon absorption studies

The two-photon action cross-sections $\eta\delta$ of two series of two-photon (TPA) dyes have been measured for excitation wavelengths throughout the wavelength range ~680-810nm, using the fs Ti:sapphire laser based setup. Two-photon fluorescence measurements were performed typically at concentrations in the range of $2x10^{-7}$M to $2x10^{-6}$ M to eliminate deviations due to re-absorption of the emitted light. Only in case of very weakly fluorescent dyes, higher concentrations were used: MH-5/dichloromethane (DCM) at $5.03x10^{-5}$M (but results were in agreement with some data points measured at $1.03x10^{-6}$M); MH-82/toluene at $7.36x10^{-5}$M. Coumarin 307 in methanol was used as the reference standard. The wavelength range accessible with the fs Ti:sapphire laser essentially only covers the region around the $S_0 \rightarrow S_1$ transition. This band gives only very low $\eta\delta$ values, suggesting that even here the $S_0 \rightarrow S_1$ transition is only weakly allowed. The obtained $\eta\delta$ values for these compounds at about 120 are quite high. The spectra are plotted in Figure 4.5.2.1.

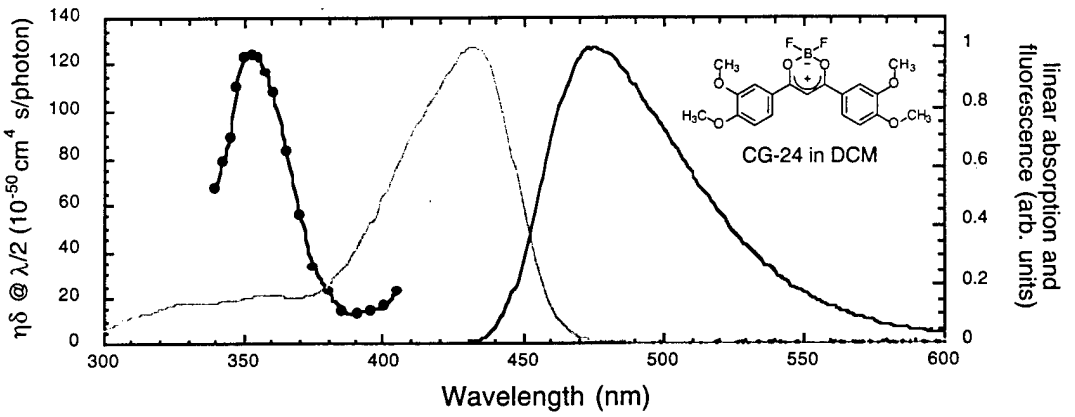

Figure 4.5.2.2a

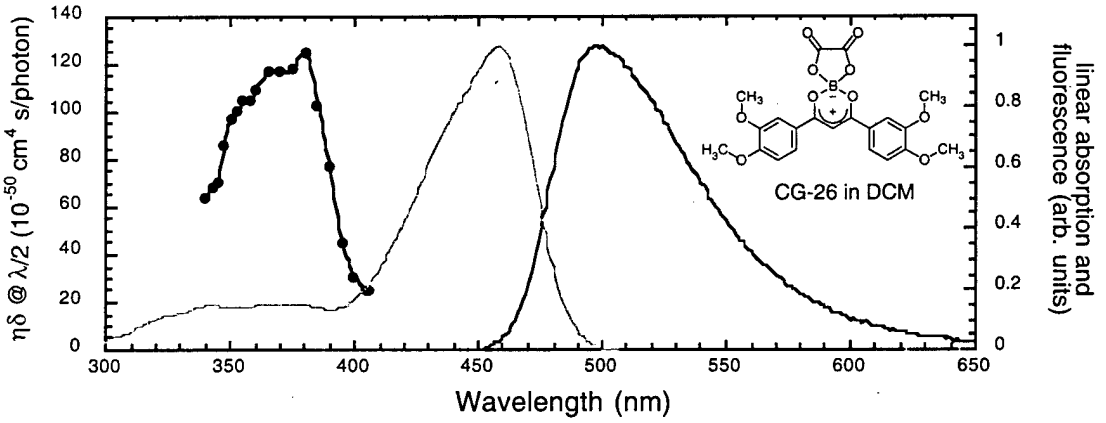

Figure 4.5.2.2b

Figure 4.5.2.2: Linear absorption (gray), one-photon-excited emission (dark gray) and two-photon excitation spectrum (black with dot) for the studied compounds. The two-photon spectrum is plotted vs. half the actual laser wavelength, for easy comparison with the linear absorption spectra for a) CG-24 and b) CG-26.

4.5.3 Electron Transport Materials

We have embarked on a program to synthesize electrochemically reversible materials that have low charge injection barriers and high mobility through: 1) improved overlap (order) between individual redox active groups by synthesis of conjugated transport materials and by synthesis of discotic LC crystals which may be subsequently crosslinked, synthesis of side chain LC polymers, synthesis of conjugated electron transporting polymers; 2) synthesis of new electronic transport molecules which contained extremely strong acceptors, preferably) bis-acceptor substituted π-conjugated materials displaying reversible electrochemistry, preferably one in which there are relatively small structural changes upon reduction (as evidenced by kinetic reversibility of electrochemical reduction, vibrational spectroscopy and X-ray diffraction studies) and which undergo reduction at potential near or lower than oxygen, to preclude oxygen acting as a trap.

Due to the electron deficient nature of dioxaborines, they are possible candidates for electron transport materials. Bis-dioxaborine **CG20** was according to Scheme 4.5.3.1.

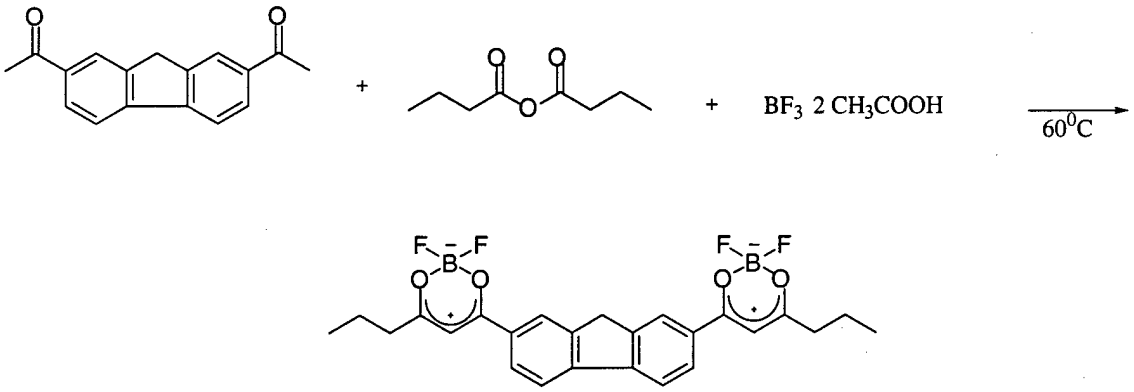

CG20

Scheme 4.5.3.1

This molecule was not an attractive candidate to be an electron transport material because it was not very soluble in common solvents which made purification difficult. In addition, this compound was very crystalline possibly due to the π- stacking interactions of the mostly flat structure of the molecule. In order to improve the solubility of the dioxaborines, synthesis of alkyl substituted fluorenes were attempted. The alkyl groups would prevent the fluorenes from aggregating thus improving the solubility. A dipentyl substituted fluorene CG22 was synthesized and then acylated via Friedel-Crafts acylation to form Scheme 4.5.3.2. This molecule was reacted

with butyric anhydride and boron trifluoride to make the corresponding dioxaborine. The resulting dioxaborine CG29 was a yellow solid (Scheme 4.5.3.3). In solution it was quite fluorescent. CG29 was substantially more soluble in dichloromethane than CG20 and was slightly soluble in ethyl acetate and acetic acid neither of which CG20 was soluble.

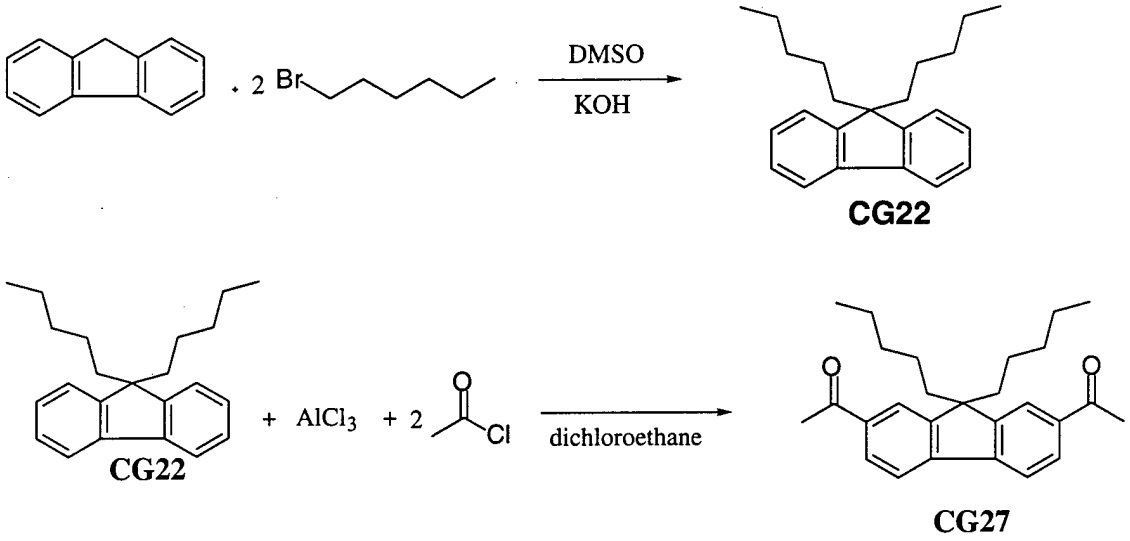

Scheme 4.5.3.2

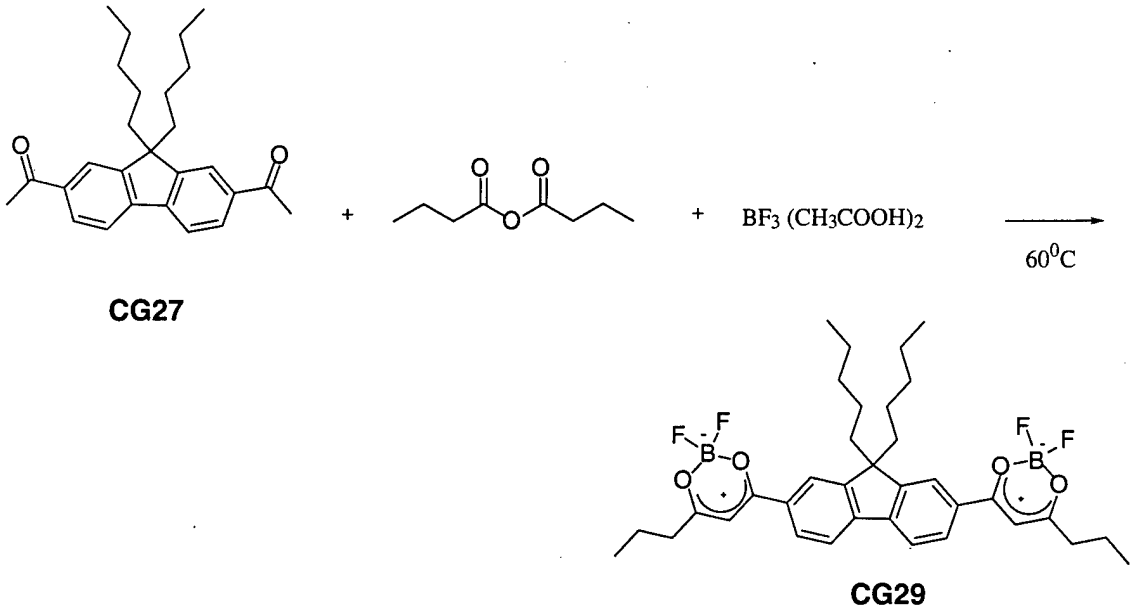

Scheme 4.5.3.3

A second alkyl a single substituted 1-methylbutylfluorene **CG28** was synthesized. The diacylated methylbutylfluorene was used to make oxaborine Scheme 4.5.3.4. The product was recrystallized from acetic acid. This product was an orange solid that fluoresced greatly in solution and in the solid state.

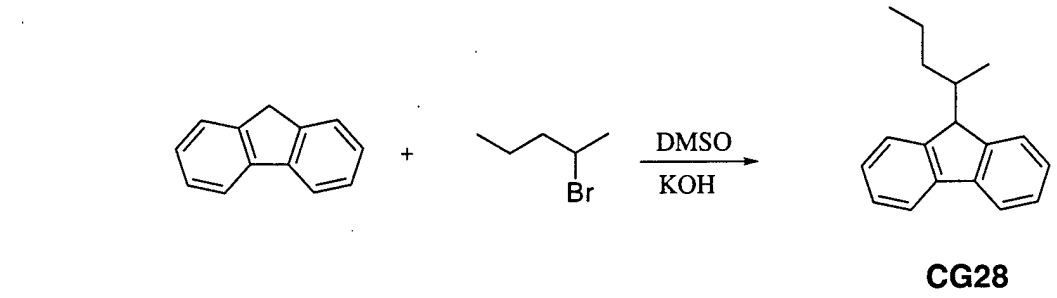

CG28

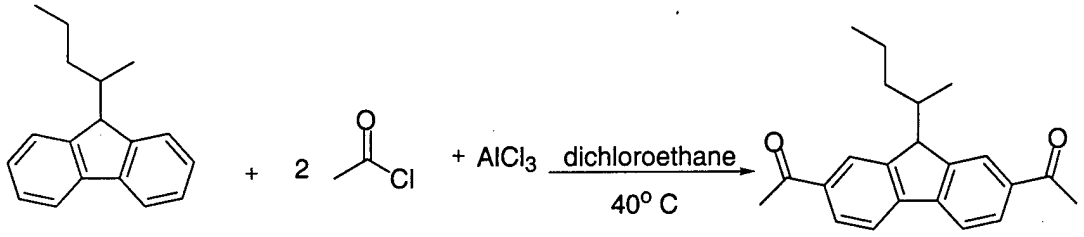

CG28 **CG31**

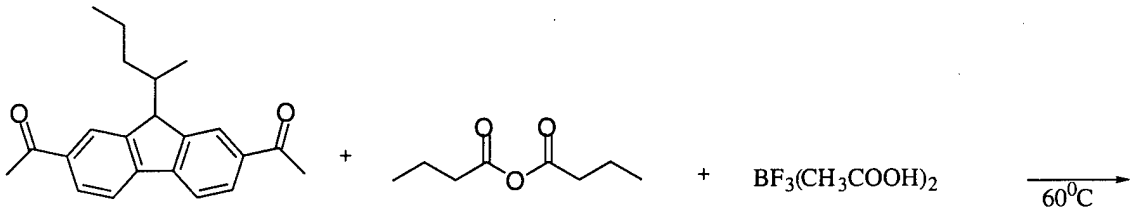

CG31

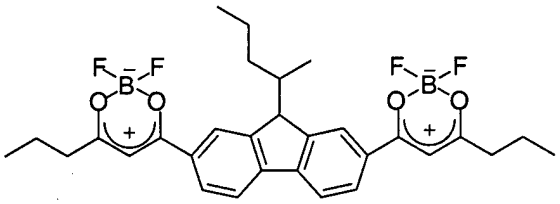

CG36

Scheme 4.5.3.4

The fluorene **CG31** was also used to make dioxaborine **CG37** which was an amorphous solid (Scheme 4.5.3.5).

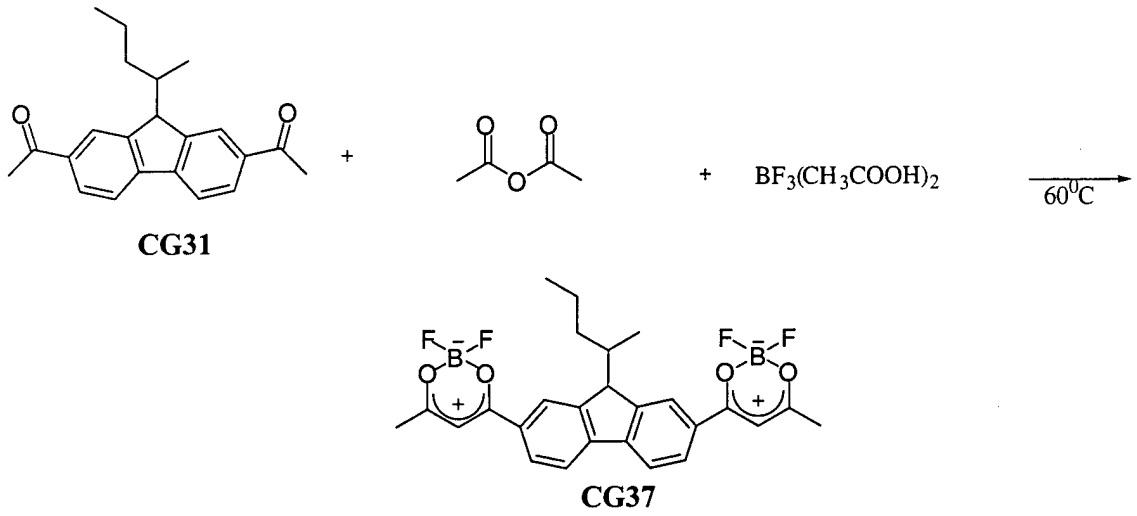

CG31

CG37

Scheme 4.5.3.5

These three compounds were all highly fluorescent with extinction coefficients around 85,000 L/mol*cm are summarized in Table 4.5.3.1. Their absorption maximums occur around 410 nm and their emission maximums occur around 425 nm.

Table 4.5.3.1 Absorption and Emission Data

Compound	Extinction Coefficient (log ε)	Absorption Max (nm)	Emission Max. (nm)
CG29	4.95	414	428
CG36	4.93	411	N/A
CG37	4.92	409	424

Differential scanning calorimetry (DSC) was performed on CG29 and CG36. CG29 had a melting point at 240°C but upon cooling did not recrystallize as evident by the lack of an exotherm. This indicates that the compound may have been in an amorphous state. The second heating of the sample has an endotherm which could be the glass transition temperature (T_g) at 70°C. Above this temperature the sample would be amorphous. Then at 160°C there is an

exotherm which could be the crystallization temperature (T_c). Finally at 210°C there is the melting temperature (T_m).

The DSC of **CG36** showed a T_g at 65°C, T_c at 120° C and T_m at 210°C in the first heating sample. Upon cooling, **CG36** does not form an ordered solid and does not have an exothermic peak. The second heating and cooling cycle is much like the first except the T_c has moved to a higher temperature.

From the work done so far these molecules, particularly **CG36**, show some promise as electron transport materials. By nature these molecules are electron deficient. In addition, the addition of the alkyl groups have made the molecules amorphous, and more soluble than **CG20** which is necessary to make them into viable devices. Preliminary results obtained in collaboration with Bernard Kippelen suggest that these compounds may be of interest as sensitizers and transport material in photorefractive composites.

4.6 Development of Dopants with Large Dielectric Anisotropy for Liquid Crystals and New Monomers for Polymeric Organic Light Emitting Diodes

Richard Hrehra, graduate student working under the direction of Dr. Seth R. Marder.

4.6.1 Dopants With Large Dielectric Anisotropy For Liquid Crystal Displays

4.6.1.1 Introduction

Molecules were synthesized to be used as dopants in liquid crystal devices. The molecules are believed to have a high dielectric anisotropy and should lower the effective switching voltage of the liquid crystal. The threshold voltage of a homogeneously aligned liquid crystal cell is given by the Freedericksz equation, $V_{th} = \Pi[K_{11}/\Delta\varepsilon]^{1/2}$. Based on this equation the threshold voltage, V_{th}, is governed by the dielectric anisotropy, $\Delta\varepsilon$, and the splay elastic constant, K_{11}. Increasing the dielectric anisotropy should therefore lower the working voltage. By lowering the working voltage low cost drivers can be used to produce liquid crystal displays with better clarity and wider viewing angles. For display applications it is desirable to have colorless dopants. Toward this end, molecules with triple bonds were synthesized as they should not absorb in the visible region of the electromagnetic spectrum.

4.6.1.2 Results

The Molecules in Figure 1 were synthesized and characterization by gas chromatography-mass spectroscopy, ^{1}H and ^{13}C nuclear magnetic resonance spectroscopy and elemental analysis.

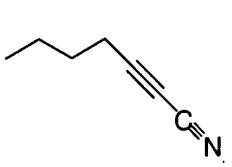

RDH-I-150

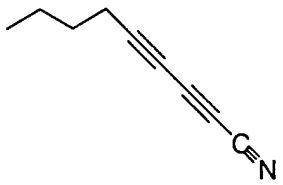

RDH-I-154

Figure 4.6.1.2.1 Acetylenic dopants for liquid crystal displays.

The reaction in Scheme 4.6.1.2.2 was performed on a 46-mmol scale.[i] The hepta-2-ynenitrile, RDH-I-150 was isolated in 31% yield. The yield was low due to the multiple vacuum distillations required to obtain the pure product.

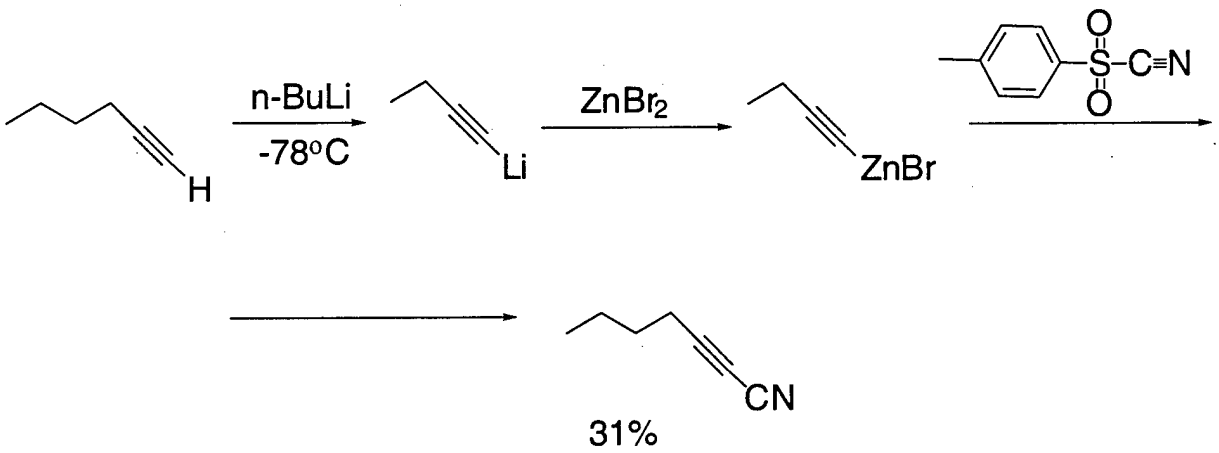

RDH-I-150

Scheme 4.6.1.2.2

The reactions in Scheme 4.6.1.2.3 were performed and the intermediates and product were isolated. The material was purified initially by vacuum distillation and then purified by repeated flash chromatography over silica gel. In each case the molecules had no absorption at wavelengths longer than 250 nm and were thus completely transparent in the visible region of the spectrum.

---

[i] Klement, I; Lennick, K; Tucker, C. E.; Knochel, P; *Tetrahedron Lett.* **1993**, *29*, 4623-4626.

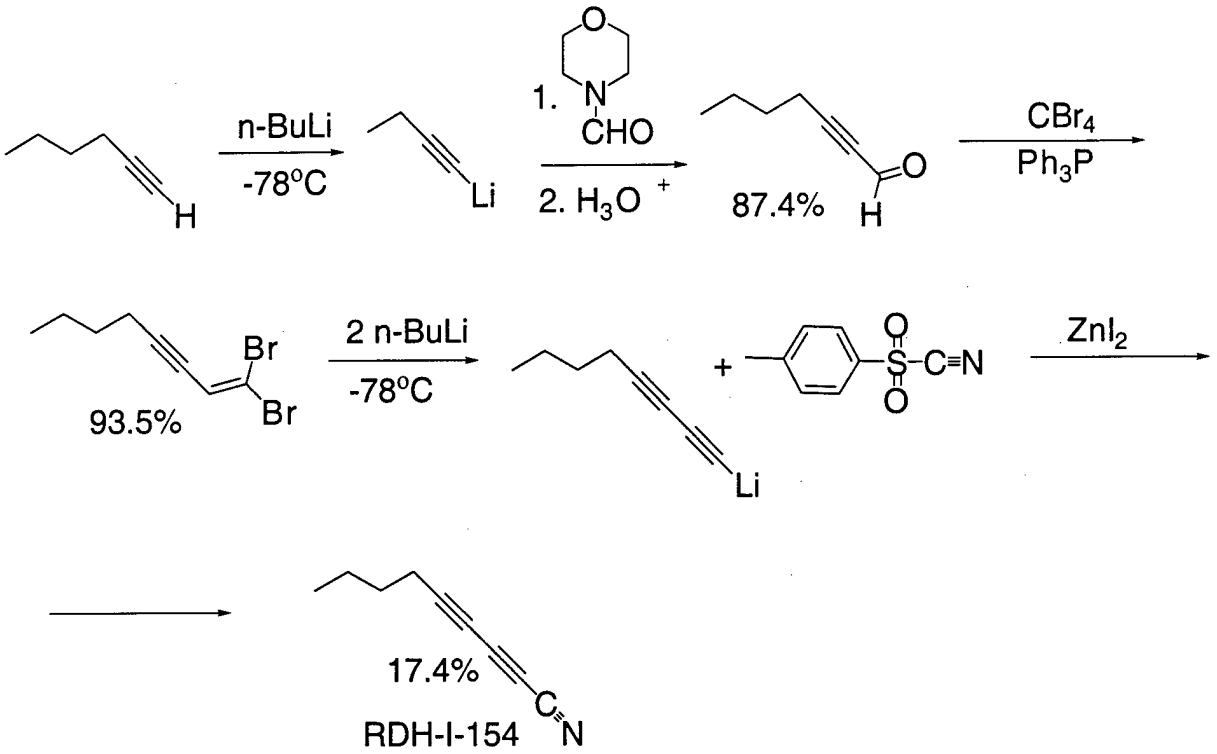

Scheme 4.6.1.2.3

The samples RDH-1 150 and RDH-1 154 were sent to Shin-Tson Wu at Hughes to provided measurements of their dielectric properties. The compounds had moderate dielectric anisotropies in the range of 9-14 comparable to standard liquid crystals and lower than some of the chromophores that we have examined previously. However, it was observed that the samples, in addition to having a moderate effect on dielectric anisotropy the dopants actually reduced the viscosity of the liquid crystal mixture. Both effects reduce the threshold voltage making molecules of this type interesting, as earlier dopants had a larger effect on dielectric anisotropy they also had the tendency of increasing the viscosity of the liquid crystal. This new class of dopants raises the possibility of manipulating two variables to achieve the greatest effect on threshold voltage.

4.6.2 New Monomers for Polymeric Organic Light Emitting Diodes

4.6.2.1. Introduction

Light-emitting diodes (LEDs) based on organic small molecules and polymeric materials[3,4] have recently attracted much attention because of their potential for use in flat panel displays. The most efficient devices to date are multilayer structures composed of hole transport, emitting and electron transport layers sandwiched between two electrodes. Incorporation of hole transport materials give the appropriate ionization potential and can lead to optimized injection and transport properties. In addition, charge carrier transport can be balanced by tuning the injection barriers leading to devices with improved efficiency. Through incorporation of the use of different substituents on a core a Bis{di[N-(phenyl)-N-(4-methylphenyl)amino]}-biphenyl, (TPD) a library of molecules with a tunable ionization potential can be generated and examined for their efficacy in OLEDs. OLEDs are generally fabricated by vapor deposition of small molecules or through the use of polymers. Polymers are often deposited by wet methods for example by spin-coating. A requirement for fabricating multilayer devices by such techniques is that application of a subsequent layer does not result in the dissolution of layers that have been applied in previous steps. One approach to circumventing this problem is to decrease the solubility of the layer subsequent to its deposition. The precursor polymer route which has been used extensively for fabrication of LEDs with a poly(p-phenylenevinylene) (PPV) system is an excellent example as such an approach. A soluble PPV precursor is coated onto indium tin oxide (ITO) substrate and thermally converted into an insoluble PPV film. Alternatively soluble polymers can be converted into insoluble polymers by either photo-crosslinking and thermal-crosslinking reactions. The photo-crosslinking technique is widely used in the casting industry and in photo-resist technology and can allow for the photo-patterning of pixels. Recently, photo-crosslinkable side-chain polymers[9,10] and low molecular weight glass compounds have been reported for organic LEDs. Thermally crosslinkable oligomers and polymers have also been reported. Here we report on the synthesis, characterization of monomer for incorporation into photocrosslinkable side-chain acrylate polymers containing triphenyldiamine as hole transport agent and cinnamate, and chalcone groups as photocrosslinking groups.

4.6.2.2Results

The target monomers can be seen in Scheme 4.6.2.2.1 have been synthesized by standard organic procedures. The HOMO levels of these monomers should vary in such a way as to bridge the barrier to hole injection for a broad variety of anode-emitting layer combinations.

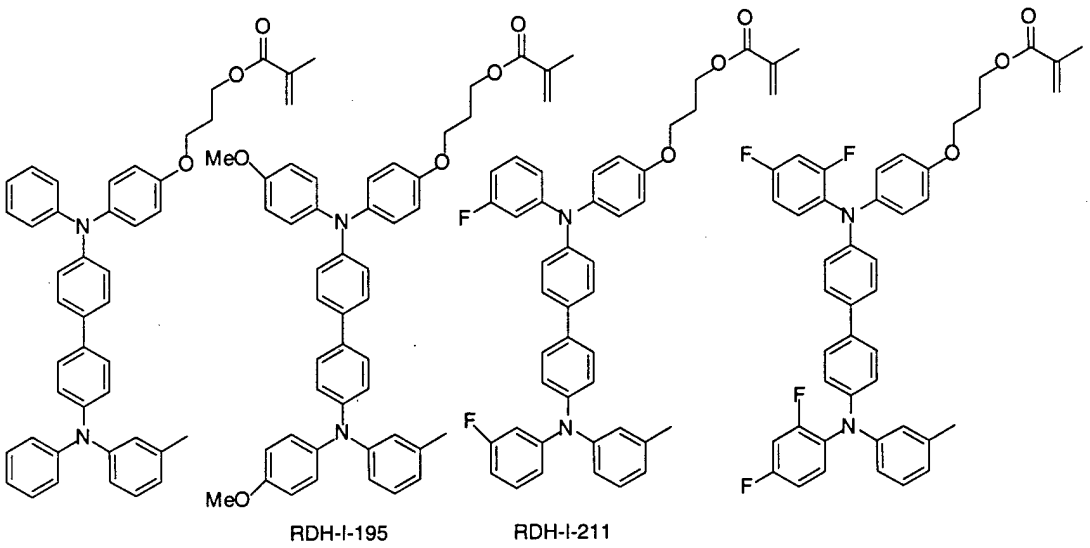

Scheme 4.6.2.2.1

4.7 Novel dicyanoketene propylene acetals as high-dipole colorless dopants to reduce the operating voltage of liquid crystal devices.

Johanna Schmidtke, undergraduate student working under the direction of Dr. Seth R. Marder.

4.7.1 Results

Low voltage operation of liquid crystal devices is highly desirable because it enables low cost electronic drivers to be used. The recently developed polymer-stabilized cholesteric displays exhibit excellent brightness and wide viewing angle. However, their operating voltage remains quite high (50 V_{th}). We aimed to utilize the potentially high dipole moment inherent in the dicyanodioxoethylene moiety incorporated in pseudo-1D molecules, to dope polymers in liquid crystal devices and thus reduce their turn-on voltage.

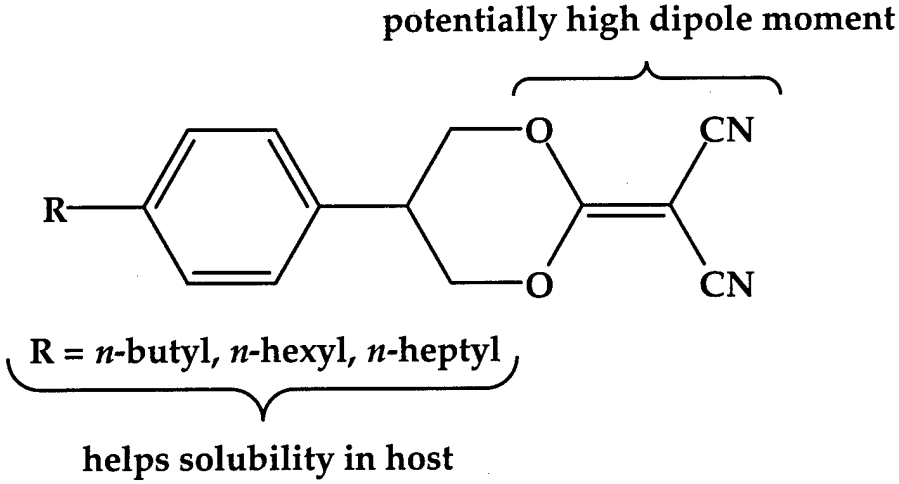

The synthesis of the dicyanoketene propylene acetals utilized the critical step wherein a diol and tetracyanoethylene were reacted together. The diols were synthesized using known literature procedures. Further studies are currently in progress.

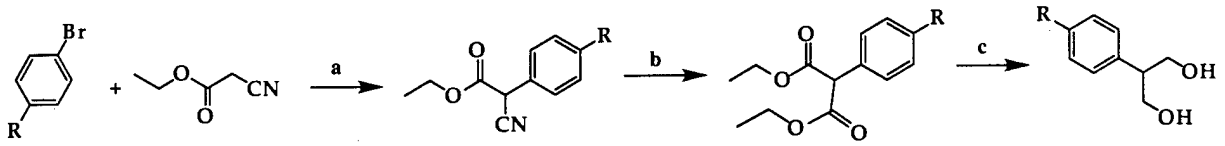

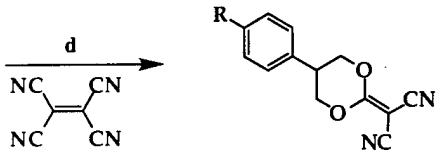

R = *n*-butyl, *n*-hexyl

a) KO^tBu, DME, $PdCl_2(PPh_3)_2$;
b) ethyl alcohol, HCl (conc), $CaCl_2$, benzene;
c) 1. $LiAlH_4$, ether, 2. ethyl acetate, 5% NaOH;
d) $NH(C_2H_5)_2$, THF

5. PERSONNEL

Michael Wagaman	Graduate Student
Lael Erskine	Undergraduate Student
Jeff Mendez	Undergraduate Student
Arjun Mendiratta	Undergraduate Student
Rick Hrehra	Graduate Student
Cara Grasso	Graduate Student
Johanna Schmidtke	Undergraduate Student

In addition, several people who are not directly receiving funding from this grant but who are performing work in a collaborative manner include:

Marguerite Barzoukas
Nasser Peyghambarian
Mireille Blanchard-Desce
Alain Fort
Alex Jen
Bernard Kippelen
Shin-Tson Wu
Joseph Perry

6. PUBLICATIONS

1. Kippelen, B.; Marder, S. R.; Hendrickx, E.; Maldonado, J. L.; Guillemet, G.; Volodin, B. L.; Steele, D. D.; Sandalphon, Y. E.; Yao, Y. J.; Wang, J. F.; Rockel, H.; Erskine, L.; Peyghambarian, N. "Infrared photorefractive polymers and their applications for imaging." *Science* (1998), 279, 54-57
2. Wagaman, M. W.; Grubbs, R. H. "Synthesis of Organic and Water Soluble Poly(1,4-phenylenevinylenes) Containing Carboxyl Groups: Living Ring-Opening Metathesis Polymerization (ROMP) of 2,3-Dicarboxybarrelenes." *Macromolecules* **30**, 3978 (1997).
3. Wagaman, M. W.; Bellman, E.; Cucullu, M.; and Grubbs, R. H. "Synthesis of Substituted Bicyclo[2.2.2]octatrienes." *Journal of Organic Chemistry*, (1997), 62, 9076-9082
4. Wagaman, M. W.; Bellmann, E.; Grubbs, R. H. "Photoluminescence properties of polynaphthalenevinylene (PNV) homopolymers and block copolymers by ring-opening

metathesis polymerization (ROMP) and study of their photoluminescence properties." *Philos. Trans. R. Soc. London, Ser. A* (1997), 355, 727-734

5. Elder, Delwin L.; Wagaman, Michael W.; Grubbs, Robert H. "Photoluminescence properties of dialkoxy poly(1,4-naphthalenevinylene) (PNV) homopolymers and copolymers synthesized by ROMP-aromatization route." *Polym. Prepr.* (Am. Chem. Soc., Div. Polym. Chem.) (1998), 39, 733-734
6. Thayumanavan, S.; Mendez, Jeffrey; Marder, Seth R. "Synthesis of Functionalized Organic Second-Order Nonlinear Optical Chromophores for Electrooptic Applications." *J. Org. Chem.* (1999), 64, 4289-4297
7. Cumpston, B. H.; Ananthavel, S. P.; Barlow, S.; Dyer, D. L.; Ehrlich, J. E.; Erskine, Lael L.; Heikal, A. A.; Kuebler, S. M.; Lee, I.-Y. S.; McCord-Maughont, D.; Qin, J.; Rockel, Harald; Rumi, M.; Wu, X.-L.; Marder, S. R.; Perry, J. W. "Two-photon polymerization initiators for three-dimensional optical data storage and microfabrication." *Nature* (1999), 398 (6722)
8. Mendiratta, A.; Barlow, S.; Day, M. W.; Marder, S. R. "Synthesis and Properties of a (Diarylamino)ferrocene and Its Radical Cation." *Organometallics* (1999), 18, 454-456

7. INTERACTIONS/TRANSITIONS

7.1 Participation at meetings, conferences, seminars

1. Marder, S. R. "*Recent Advances in the Design and Use of the Real and Imaginary Third-Order Optical Nonlinearities of Organic Dyes*" Presented at The Third International Conference on Organic Nonlinear Optics, Marco Island, FL, December 15-20, 1996.

2. Marder, S. R. "*Nonlinear Absorbing Chromophores.*" Presented at the American Physical Society National Meeting, Kansas City, MO, March, 16-21, 1997.

3. Marder, S. R., "*Optimizing the Real and Imaginary Third-Order Optical Nonlinearities of Organic Molecules.*" OPTIMAS Workshop on Nonlinear-Optical Properties of Polymers and Related Topics, Bayreuth, Germany, June 30- July 1, 1997.

4. S. R. Marder, "*Design and Applications of Molecules with Large Multiphoton Absorption Cross Section*" NATO Advanced Research Workshop, Menton, France, August 26-29 1999

7.2 Consultative and advisory functions

None.

7.3 Transitions

1 Polyphenylene-vinylene polymers have been transitioned to Nasser Peyghambarian and Bernard Kippelen (University of Arizona) for testing in organic LED devices.

2. Substituted triphenylamino donors with either aldehyde or bromide functionality have been transitioned to Larry Dalton (USC) for incorporation in highly nonlinear, stable electro-optic polymers.

8. NEW DISCOVERIES

None

9. HONORS/AWARDS

1995-1999	S. R. Marder, Member, Board of Reviewing Editors for *Science.*
7/67 - 6/99	S. R. Marder and J. W. Perry, NSF Special Creativity Award Extension